On the relation between geometric and flow properties of a miniaturized fluid oscillator

J. O. Sotero-Esteva[1], R. Furlan[2] & J. J. Santiago-Avilés[3]
[1]*Department of Mathematics,*
University of Puerto Rico at Humacao, Puerto Rico
[2]*Department of Physics and Electronics,*
University of Puerto Rico at Humacao, Puerto Rico
[3]*University of Pennsylvania, Philadelphia, USA*

Abstract

A miniaturized fluid oscillator with no movable parts composed by a switching cavity, one inlet, two outlets and two feedback channels was studied. Examples of these devices have been built before and had shown oscillation of fluid flows ranging from tens of Hz for liquids to thousand of Hz for gases. The present work consists of a study of the flow within the device by means of a computer model. The computer model was built using COMSOL 3.3. It uses conventional Navier-Stokes equations numerically solved by Finite Element Methods. A new level of detail of the qualitative description of the flow within the device is achieved which allows for a better understanding of why some geometries produce better devices than others. It shows that homogeneous oscillation, not only depend on the direct force exerted by the feedback flow on the inlet stream, but also on the disruption of the Coanda's effect that diverts the stream towards one of the output channels. On the other hand, the quantitative part of the study serves to validate the simulation as well as a basis for proposing new empirical models. The quantitative measurements are consistent with a previously known mathematical model that describes the relation between frequency, input velocity and geometrical and physical properties. Ongoing testing with actual devices also supports the proposed operating mechanisms and models.
Keywords: fluidic, flow control, flow meter, fluidic oscillator, finite element method, computer simulation.

WIT Transactions on Modelling and Simulation, Vol 46, © 2007 WIT Press
www.witpress.com, ISSN 1743-355X (on-line)
doi:10.2495/CMEM070311

1 Introduction

The miniaturized oscillator studied here is a structure without movable parts composed of cavities and channels. It can be used for flow control, flow measurement, and substance identification. They find applications in the areas of medicine, aeronautics and automotive industries among others. The use of macro sensors and actuators based on several designs of these oscillators can be traced back to 1960 when the demands for reliable controls for space and marine environments stimulated research in this area. A patent for a substance identification device using oscillators very similar to the one studied here was filled in 1963 and issued in 1966 [9].

The use of oscillators for the mentioned applications depend on relating their frequency response to factors such as the composition of the fluid, temperature, volumetric flow and variations in geometrical and other physical properties of the device. Most of the characterizations of fluidic devices found in the literature are based on experimental methods where actual devices are made and tested by varying the desired parameters. Most frequently the factors that are studied are those that require building one or a few devices for all tests. To study of the effect of geometry variations in the laboratory gets complicated by the fact that the researcher would have to build and test dozens, or perhaps hundreds, of devices.

Up until recently computational testing methods were difficult to use as well. Limited software tools for numerical computations and visualization, lack of processor speed, and limitations in the mathematical modeling severely restricted the use of the computer for the study of these devices. Software libraries and simulation environments for solving systems of differential equations based on Finite Element Methods (FEM) such as FreeFem, ANSYS and COMSOL, among others, are now mature enough for such complex simulations. They have excellent visualization capabilities, automatic initial and adaptive meshing, scripting for automatic geometry design and graphical user interface (GUI) generation, and even parallel processing capabilities.

In a "V" shaped device without feedback arms in which the inlet is placed at the junction and the outlets at the end of the upper arms the fluid flow tends to stick to one of the lateral walls due to the Coanda's effect. Fluid emerging from the inlet creates a partial vacuum just after entering to the switching chamber. A fluid vortex is formed in this low pressure region.

The miniaturized fluid oscillator with no movable parts studied in this work is composed by a switching cavity, one inlet, two outlets and two feedback channels (see figure 1). The feedback channels divert part of the flow back to the junction, switching the flow to the other arm where the same event is repeated, thus creating the oscillations. Experimental results indicate that the operation of this type of fluid oscillator is a direct function of the length of the feedback loops and of the velocity inside of the interaction region. The main oscillation frequency modes range from tens of Hz for liquids (water, isopropyl alcohol and

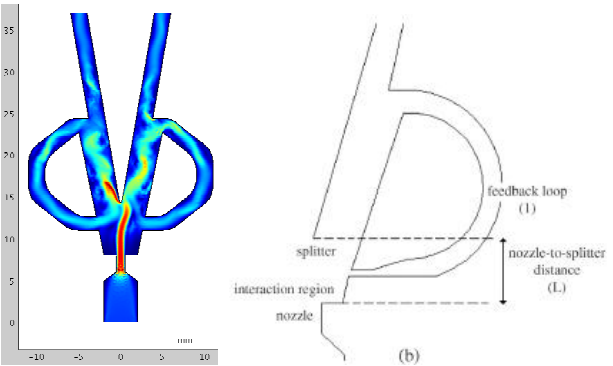

Figure 1: A feedback fluid oscillator with one inlet nozzle, two feedback loops and two output channels.

acetone) to thousand of Hz for gases (nitrogen, argon, and carbon dioxide) [7]. Experimental evidence of internal flow oscillation with operation with water has also been reported in [5].

Simões *et al.* [8] analyzed a feedback oscillator numerically using ANSYS 5.7. They studied variations in fluid properties and proved the viability of using FEM based numerical methods for the simulation of fluid flow in these devices. This work is a computational study on how the positions and width of the feedback arms affect the oscillation patterns when water flows through the channels at low input speeds (< 200mm/s). All other geometry parameters are kept constant.

2 Analytical modelling

For subsonic or transonic flow, associated with quasi-laminar or turbulent regime, the frequency of oscillation is determined by: the time of interaction of the fluid in the feedback loop (τ_f), by the amplifier switching dynamics (τ_s), and by the flow-rate (u). In this case, the typical feedback oscillator can be designed to give a long linear range of frequency against velocity characteristics.

The total oscillation time is described as in [8] as $T = 2(\tau_f + \tau_s)$. The feedback transmission time is $\tau_f = l / c$ where, c is the wave propagation speed, l is the feedback loop length. The switching time is $\tau_S = \xi R / u$ where u is the jet velocity, R is the nozzle to splitter distance, and ξ is an empirical constant. If the duct is not small, the speed of wave propagation tends to the speed of sound. For liquids the speed of wave propagation is two to four orders of magnitude higher than the jet velocity in the nozzle-to-splitter path. Therefore, for a fixed geometry the following linear relation between frequency and input fluid speed holds:

$$f = \frac{1}{2\tau_S} = \frac{\xi}{2R} u \,. \tag{1}$$

The oscillator frequency increases linearly with increasing volume flow. This behavior allows using of the feedback fluid oscillator for the measurement of the flow of Newtonian fluids.

A feedback oscillator may exhibit many oscillation frequency modes. The conditions under which a device exhibits few modes is crucial for many applications. In this work the term *properly designed device* refers to a device in which the number of dominant oscillatory modes is low. Ideally, an oscillator should have only one dominant mode. Equation (1) describes a system with only one oscillation frequency; it implicitly assumes a properly designed device. Since the apparent flow in the switching cavity is far more complex than in the feedback arms, closely studying what happens inside the switching chamber is a crucial step in the design of properly crafted oscillators.

3 Simulation procedure

In order to simplify the computational effort a two dimensional model was used. The validity of the simplification is justified by the aspect ratio used in actual devices. The computer model was built using COMSOL 3.3 running on a Silicon Graphics Altix 350 with eight Itanium2 processors. Navier-Stokes equations were numerically solved by Finite Element Methods.

3.1 Mathematical model

The incompressible Navier-Stokes equations [1, 11],

$$\rho\frac{\partial u}{\partial t}+\rho u\cdot\nabla u=\nabla\cdot\left[-pI+\eta\left(\nabla u+(\nabla u)^{T}\right)\right],$$

$$\nabla\cdot u=0,$$

where used. The density and the dynamic viscosity were set to $\rho = 1000$ kg/m³ and $\eta = 0.001$ kg/ms respectively, p is pleasure and I is the identity matrix. These are values commonly used in simulations of water when variations due to temperature and other factors are not to be considered. No force field and no-slip boundaries were used. Zero pressure was initially set at the output boundaries and inward velocity u_{in} at the input boundary.

3.2 Geometry

The geometries are designed to resemble those used at previous experiments with actual devices (figure 2). The feedback channels have a constriction at the return joint that varies from 0.04mm to 2mm. The separation from the base of the switching chamber varies from 0mm to 4mm in 1mm increments. The rest of the dimensions are kept fixed. The input, output and feedback channels have a width of 2mm.

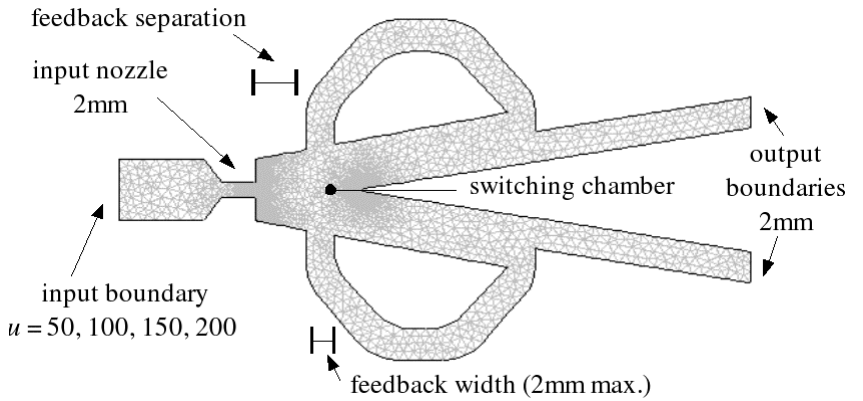

Figure 2: Geometry, measurements, and distribution of triangles throughout the mesh.

The mesh used was generated by COMSOL 3.3. It is a triangular mesh with higher density of vertices around borders with high curvature. The distribution of vertices is neither uniform nor symmetric. The maximum length of a triangle edge in the mesh varied. A maximum of 1mm (shown in figure 2) was used for smaller flow rates. Denser meshes were used for higher flow rates. A Delaunay triangulation was adopted.

3.3 Simulation parameters

A series of test runs were performed with a duration of three seconds of simulated time. From those tests it was determined that all devices that showed oscillations after one second were most likely to continue oscillating until the end of the test run. It was inferred that when a test case pass this point it is most likely to exhibit *persistent oscillations*, that is, it will keep oscillating during an arbitrary long period of time. It was also observed in the test runs that oscillatory behavior usually stabilized before that moment and that 1.5s of simulated time gives sufficient data to capture the main oscillation modes of the device. Simulated data was produced for 25 different geometries. Input fluid speed ranged from 50mm/s to 300mm/s in 50mm/s increases for a total of 150 runs of the simulation. The maximum fluid speed at the end of the output channels was measured every 0.05s. The transient analysis was performed using a default element type Lagrange P_2P_1, the state of the system is stored every 0.05s of simulated time.

3.4 Post-processing

Two graphs were produced for each simulation. The first one is a plot of time versus the differences between maximal output fluid velocities at the end of the output channels at that time. The second was the Fourier Transform of the

previous graph that gives information of the different oscillations modes of the device. The frequencies of the three most conspicuous peaks of this graph were registered.

3.5 Computational tools

COMSOL Script was adopted in order to speed up the simulation process, allowing a more complete analysis of the influence of geometry of the device. Modules for geometry generation, definition of the model, automatic calling of meshing functions, setting of the model, time-dependent simulation functions and post-processing were written (see [9] for details). Those scripts were also useful for batch processing. A Graphical User Interface (GUI) was built on top of the modules (figure 3). The GUI integrates all previous functions and made possible a faster setup and manipulation of the simulation, especially for closer inspection of interesting geometries.

.

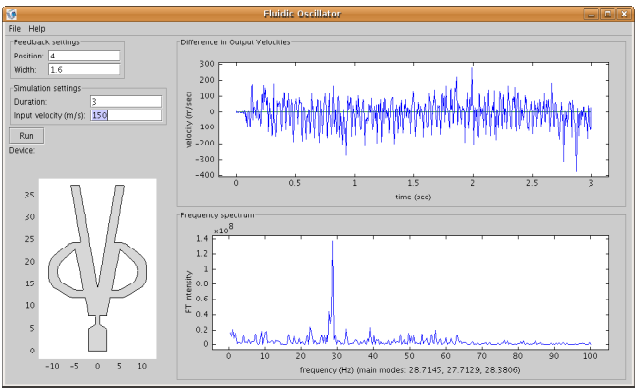

Figure 3: A Graphical User Interface (GUI) for feedback oscillator simulations and analysis.

4 Results and discussion

The discussion of results is organized in order of increasing detail. Each section considers a subset of the cases of the previous section.

4.1 Persistent oscillations

All geometries exhibited persistent oscillations at the lowest volumetric flow tests (50mm/s). No persistent oscillations were found for input speeds over 200mm/s. In all cases in which the simulation stopped before the 1.5s mark a small and highly turbulent region that caused excessive numerical instability appeared when the simulation stopped. The position of that region does not seem to follow a pattern. Attempts were made to extend the simulation time on those cases for longer periods by refining and/or adapting the mesh but were

unsuccessful. A mathematical model that accounts for turbulence, such as the κ-ε turbulence model, could produce longer simulations. But turbulence and patterns sometimes appear together in the same physical system [3], sometimes do not. The failure to converge in some cases may also reflect that there exist some combinations of properties that separate the devices in which both turbulence (oscillation) and pattern (persistence) appear from those where they do not appear

The count of cases that showed persistent oscillations shown in table 1 is evidence against designing devices with a combination of wide feedback channel close to the inlet channel.

Table 1: Number of devices with persistent oscillations.

separation	feedback width (mm)					
(mm)	0.4	0.8	1.2	1.6	2	total
0	3	1	1	1	1	7
1	3	1	1	1	1	7
2	3	1	1	2	2	9
3	3	3	3	3	3	15
4	2	2	2	3	3	12
total	14	8	8	10	10	50

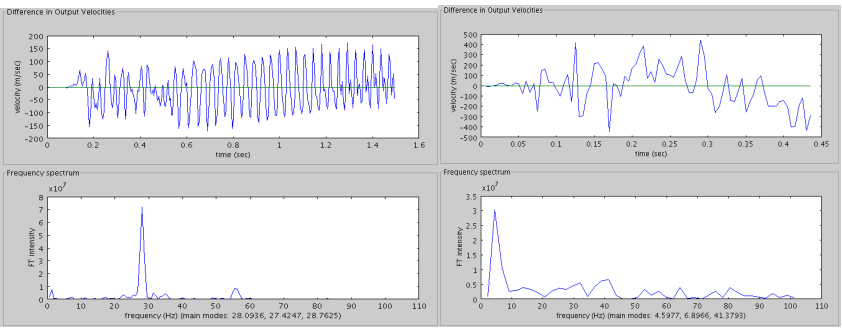

(a) (b)

Figure 4: Oscillations and frequency analysis of a (a) non-persistent oscillator device and a (b) device classified as properly designed.

4.2 Oscillation frequency modes

A variety of oscillation patterns were observed in cases with persistent oscillations (figure 4). For each case, the six highest values of discrete Fourier transform amplitudes and their corresponding frequencies were tabulated. The main oscillation frequency was determined by selecting the frequency corresponding to the highest amplitude after discarding very low frequency modes (less than 5Hz). Averages over all the different geometries were

calculated for each input velocity. The graph of input velocity versus frequency (figure 5) shows an excellent agreement with the linear model in eqn (1) and the experimental observations. The variance in the data captures experimental noise as well as small variations produced by the changes in geometric measures.

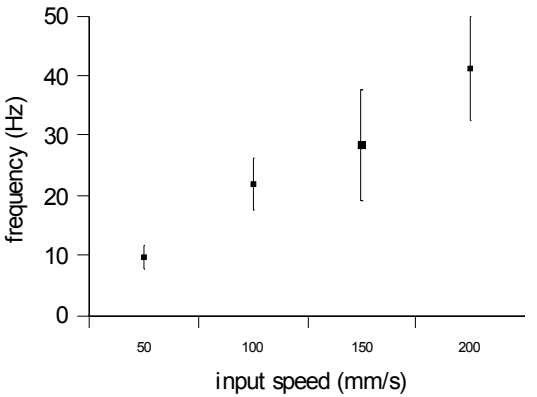

Figure 5: The average frequency in all devices with persistent oscillations. The bars cover one standard deviation from the averages.

Table 2: Properly designed devices by feedback separation and width.

separation	feedback width (mm)					
(mm)	0.4	0.8	1.2	1.6	2	totals
0	0	0	0	0	0	0
1	2	0	0	0	0	2
2	0	0	0	0	0	0
3	0	1	1	2	2	6
4	0	0	1	1	0	2
totals	2	1	2	3	2	10

4.3 Proper designs

As stated earlier, we define *properly designed oscillator* as an oscillator that has few dominant oscillatory modes; ideally only one such as the one in figure 4(b). The quantitative criterion used for classifying a geometry as a proper design was as follows: the value of the frequency for which the second highest discrete Fourier transform is less than half of the most dominant one. Ten devices satisfied the criterion (table 2)

4.4 Analysis of vorticity

A closer inspection of the vorticity plots in the switching chamber reveals details of the physical mechanisms that determine why some combinations of geometries and input velocities perform better than others. As seen in figure 6,

when the feedback arms are positioned where the eddy responsible for the Coanda's effect is located, the feedback flow not only exerts a force on the inlet stream but also disrupts the effect that keeps the jet attached to that wall.

5 Conclusions

From the analyses presented above the following conclusions are drawn about a feedback fluid oscillator. Proper positioning and width of the feedback channel are important in the design of the devices. The proper adjustment of these parameters leads to devices with a well defined oscillating framework. Homogeneous oscillations, not only depend on the direct force exerted by the feedback flow on the inlet stream, but also on the disruption of the Coanda's effect. Linear dependence between frequency and volumetric flow was confirmed for simulated water.

Figure 6: Vorticity in the switching chamber of a properly designed feedback oscillator. Light shades indicate counter-clockwise rotation, darker shades indicate clockwise rotation. The arrows show the direction and magnitude of the velocity of the fluid at the middle of the feedback arm when entering the switching chamber.

Acknowledgements

This work was supported by the US National Science Foundation through the *Penn-UPR Partnership for Research and Education in Materials* project (NSF-DMR-353730) and by the US National Security Agency through the *Humacao Undergraduate Research in Mathematics to Promote Academic Achievement* program (NSA-H98230-04-C-0486).

References

[1] Chorin, A.J. & Marsden, J.E., *A Mathematical Introduction to Fluid Dynamics*, Second Edition, Springer-Verlag: New York, 1990.
[2] COMSOL 3.3 User's Guide and Introduction, Comsol AB, Sweden, 2006.

[3] Field, M, & Golubitsky, M., *Symmetry in Chaos, A search for Pattern in Mathematics, Art and Nature*, Oxford University Press: Oxford, 1992.
[4] Gebhardy, U., Hein, H. & Schmidt, U., Numerical investigation of fluidic micro-oscillators, *J. Micromech. Microeng*. 6 (1996) 115–117.
[5] Rogerio Furlan, Maria Lucia Pereira da Silva, Eliphas Wagner Simoes, Roberto Eduardo Bruzetti Leminski, Jorge J. Santiago Aviles, Visualization of internal liquid flow interactions in meso planar structures, *Flow Measurement and Instrumentation*, Vol. 17, No. 5, pp. 298-302, 2006.
[6] Gregory, J.W., Sullivan, J. P., Raman, G. & Raghu, S., Characterization of a micro fluidic oscillator for flow control, *2nd AIAA Flow Control Conference*, Portland Oregon, June 28 – July 1, 2004, paper 2692.
[7] Simões, E.W., Furlan, R., Pereira, M.T., Numerical analysis of a microfluidic oscillator flowmeter operating with gases or liquids, *Technical Proceedings of the Fifth International Conference on Modelling and Simulation of Microsystems, MSM 2002*, ISBN: 0-9708275-7-1, pp. 36–39, 2002.
[8] Simoes, E.W., Furlan, R., Leminski, E.B., Gongora-Rubio, M.R., Pereira, M.P., Morimoto, N.I. & Santiago-Aviles, J. J., Microfluidic oscillator for gas flow control and measurement, *Flow Measurement and Instrumentation*, Vol. 16, Issue 1, pp. 7–12, 2005.
[9] Sotero Esteva, J.O., Furlan, R., Santiago Avilés & J.J., Simulation of miniaturized fluidic oscillators using COMSOL Script, Proceedings of the *COMSOL Users Conference 2006*, Boston, 2006.
[10] Testerman, M.K., McLeod Jr., P. C., Fluid oscillator analyzer and method, US Patent Office, patent #3273377, 1966.
[11] Zienkiewicz, O.C., Taylor, R.L. & Nithiarasu, P., *The Finite Element Method for Fluid Dynamics*, 6th edition, Elsevier Ed., Oxford, 2005.